

RESEARCH

Open Access



Fragment merging approach for design, synthesis, and biological assessment of urea/acetyl hydrazide clubbed thienopyrimidine derivatives as GSK-3 β inhibitors

Joseph S. Saleh^{1*}, Soha R. Abd El Hadi^{1*}, Hany S. Ibrahim¹, Eman Z. Elrazaz² and Khaled A. M. Abouzid^{2*}

Abstract

New thienopyrimidine derivatives were designed and synthesized as GSK-3 β inhibitors based on the structure of active binding site of GSK-3 β enzyme. In this study, compounds **6b** and **6a** were found to be moderate GSK-3 β inhibitors with IC_{50s} 10.2 and 17.3 μ M, respectively. Molecular docking study was carried out by docking the targeted compounds in the binding site of the GSK-3 β enzyme using the MOE program. Moreover, ADME study was performed to predict certain pharmacokinetic properties. The results showed that all synthesized compounds may not be able to penetrate the blood brain barrier; so, the chances of CNS side effects are predicted to be low. CYP1D6 is predicted to be inhibited by compounds (**5a**, **5d**, **6a**, **9a** and **9b**), So drug-drug interactions are expected upon administration of these compounds.

Keywords Thienopyrimidine, GSK3 β , Gewald reaction, Acetyl hydrazide, Docking

*Correspondence:

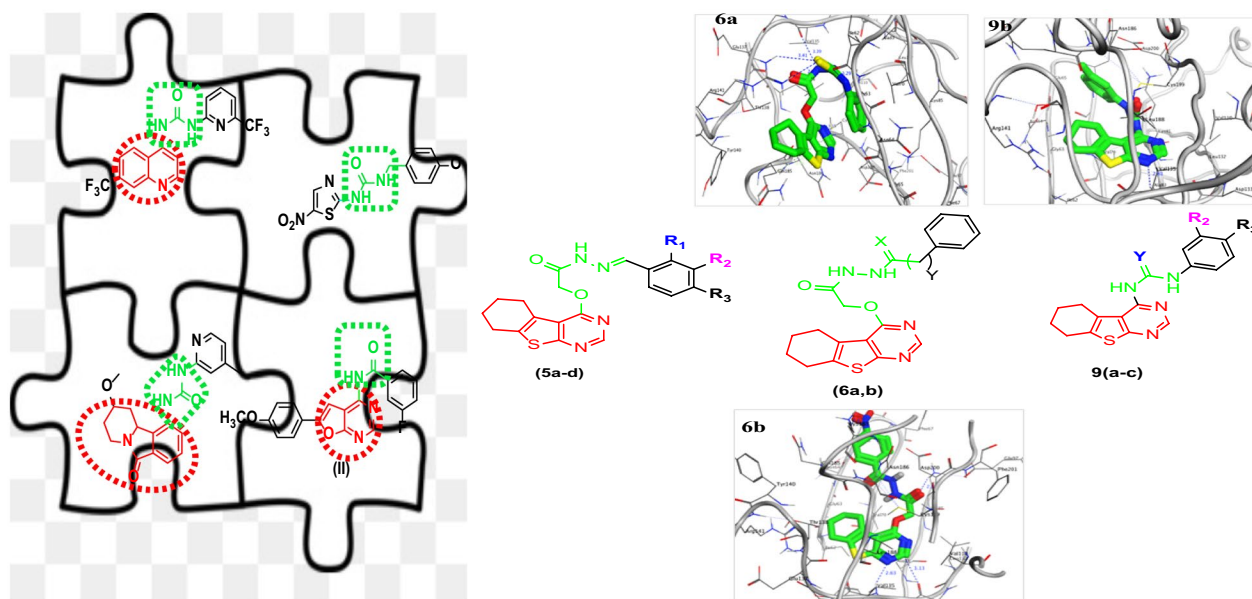
Joseph S. Saleh
Josephsamir@eru.edu.eg
Soha R. Abd El Hadi
Soha-ramadan@eru.edu.eg
Khaled A. M. Abouzid
khaled.abouzid@pharma.asu.edu.eg

Full list of author information is available at the end of the article



© The Author(s) 2023. **Open Access** This article is licensed under a Creative Commons Attribution 4.0 International License, which permits use, sharing, adaptation, distribution and reproduction in any medium or format, as long as you give appropriate credit to the original author(s) and the source, provide a link to the Creative Commons licence, and indicate if changes were made. The images or other third party material in this article are included in the article's Creative Commons licence, unless indicated otherwise in a credit line to the material. If material is not included in the article's Creative Commons licence and your intended use is not permitted by statutory regulation or exceeds the permitted use, you will need to obtain permission directly from the copyright holder. To view a copy of this licence, visit <http://creativecommons.org/licenses/by/4.0/>. The Creative Commons Public Domain Dedication waiver (<http://creativecommons.org/publicdomain/zero/1.0/>) applies to the data made available in this article, unless otherwise stated in a credit line to the data.

Graphical Abstract



Introduction

Cancer is a genetic disease with two main characteristics: uncontrolled growth of the cells and tissue invasion/metastasis of the tissues [1]. Cell cycle control is dependent on the four stages (G1, S, G2, M). A variety of metabolic pathways have been identified as critical processes for the start of a certain cell cycle event [2]. In these biochemical pathways, many protein kinases are active and employ regulated phosphorylation processes to relay biological information to downstream signaling pathways [3]. Glycogen Synthase Kinase-3 (GSK-3) is a multitasking serine/threonine protein kinase because of its broad participation in different signaling pathways [4]. GSK-3 is a cyclin-dependent kinase (CDK) proline-directed kinase, which also includes mitogen-activated protein kinases (MAPKs), cyclin-dependent kinases (CDKs), and CDK-like kinases (CLKs). GSK-3 α and GSK-3 β that encode 51 and 47 kDa proteins, respectively. Both isomers are found in cells and tissues, and their physiological activity is similar. The most common isoform is GSK3 β which overexpressed in different human cancer, that why it considers as strong therapeutic target [5]. It is a kinase that belongs to the phosphotransferase family. Originally thought to control glycogen synthase, it is now shown to phosphorylate a huge variety of substrates, hence regulating a large range of biological activities, involving Wnt and Hedgehog signaling, transcription,

and the insulin system [6]. Despite structural similarities between two isoforms, their roles are distinguished by phosphorylation at unique locations. For the activation of GSK 3 α and GSK 3 β , Tyr 279 and Tyr 216 are two sites situated at the T-loop of GSK 3 (activation domain) and are phosphorylated by upstream signaling molecules. Obviously, GSK 3 α and GSK 3 β are inhibited by site-specific phosphorylation, which is closely regulated by a variety of processes. All of these pathways for GSK3 α inactivation at Ser21 and GSK 3 β at Ser9 have been linked to the phosphoinositide3 kinase (PI3K) dependent mechanism. Activation of PI3 kinase, protein kinase A (PKA), and protein kinase B (PKB) (also termed as Akt), protein kinase C (PKC) and p90Rsk contribute to GSK3 inactivation. Inactivation of GSK 3 β is also implicated in glycogen production, protein synthesis, cell invasion and cell proliferation. Consequently, GSK 3 β is regarded as a possible therapeutic target in cancer therapy.

Recently, many GSK-3 β kinase inhibitors have been discovered that involve the quinazoline, quinoline, pyrrolopyrimidine, and furopyrimidine frameworks. These cores are thought to be a configuration that is preferred for suppressing ATP-dependent kinases. Pyrrolopyrimidine derivative (I) a promising GSK-3 β inhibitor which inhibit proliferation and cytokine production in human lung cancer (IC_{50} = 30 nm) [7]. Moreover, another bioisosteric furopyrimidine derivative (II) shows IC_{50} > 35 μ M

on GSK-3 β [8]. On the other hand, quinoline derivative (III) also inhibits GSK-3 β with $IC_{50} < 10$ nm [9]. Tricyclic tetrahydropyridoisoindolone derivative (IV) as GSK-3 β inhibitor with $IC_{50} = 0.032$ μ M [10]. Also, thiazole derivative (V) containing urea moiety has shown $IC_{50} = 2.7$ nm against GSK-3 β and used as antidepressants and also as mood stabilizer [11]. Motivated by the aforementioned facts, design novel GSK-3 β inhibitors with higher activity is a promising targeted approach in treatment of cancer [12] (Fig. 1).

Rationale and design

The structural study of GSK-3 β inhibitors were observed certain interactions between to the ATP binding site via hydrogen bonds with Asp133 or Val135 (two key binding residues) [13]. Based on the urea moiety's substituent, we revealed two distinct mechanisms of binding. The first one, in the tetrahydropyridoisoindolone scaffold where the carbonyl group in one binding mode directs towards the catalytic Lys85, whereas the urea is parallel to the hinge area, forming a hydrogen bond contact between the urea and the backbone of Val135. In GSK3 β , a second method of binding was more discovered. In the tetrahydropyridoisoindolone scaffold, the carboxyl group binds with the NH backbone of Val135 by a hydrogen link, and the catalytic Lys85 interacts with the urea via a hydrogen bond. If the ortho position contains nitrogen, the heterocyclic scaffold connected to the urea can form a further hydrogen bond with Lys85. The substituent connected to the saturated ring of the tetrahydropyridoisoindolone scaffold interacts with Thr138 through a hydrogen bond

network or a van der Waals interaction, depending on the orientation of the residue side chain [14, 15]. According to the level of potency, activity of pyrrolopyrimidine (I), furopyrimidine (II), quinoline derivative (III) and tetrahydropyrido[1,2-a]isoindolone (IV) as GSK-3 β inhibitors have IC_{50} in micromolar or nanomolar range, ring replacement of pyrrolopyrimidine and furopyrimidine with thienopyrimidine core to explore additional interaction with the hinge region of kinase.

The goal of this work was to provide evidence to support the use of thienopyrimidine scaffold as a pharmacophoric constituent essential in the development of novel GSK-3 β inhibitors [16]. In this study thienopyrimidine scaffold was utilized to design novel GSK-3 β kinase inhibitor depending on the main reasons: novelty of this fragment because it is not exploited yet in any clinically approved drug. Also, tetrahydrothienopyrimidine can be readily synthesized from commercially available materials. Based on the aforementioned findings, fragment merging approach and structure extension through linking the urea moiety or amide moiety with thienopyrimidine scaffold to explore if occupy a deep hydrophobic allosteric pocket. As a result, several substitution patterns on (R) on the terminal phenyl ring were studied to investigate the interaction with the terminal allosteric pocket (Fig. 2).

Results and discussion

Chemistry

Scheme 1 offered synthesizing methods for targeted compounds. The appropriate intermediates, which were

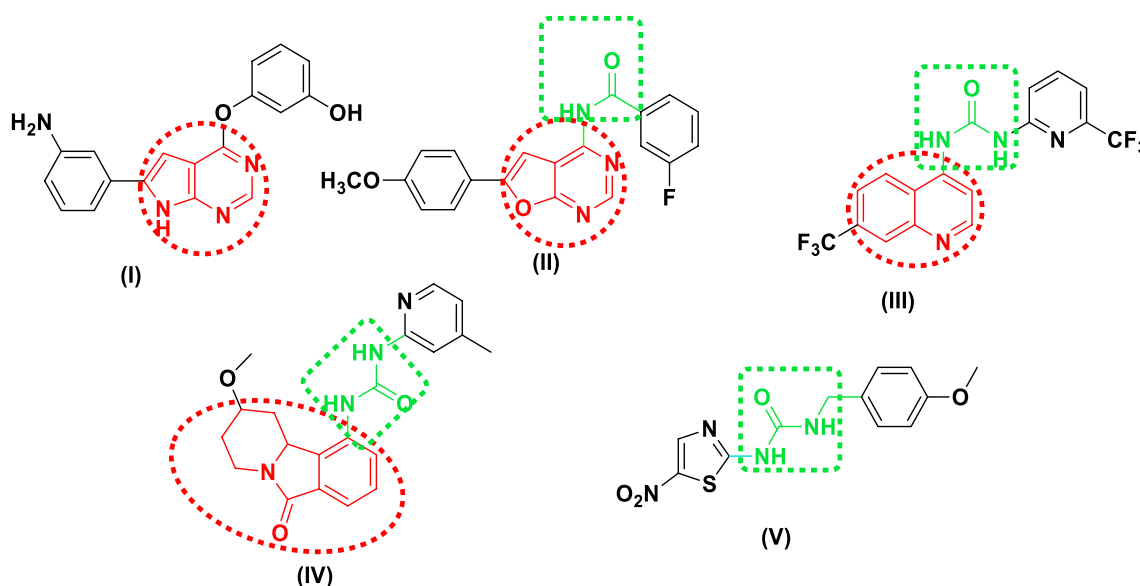


Fig. 1 Some reported GSK3 β inhibitors

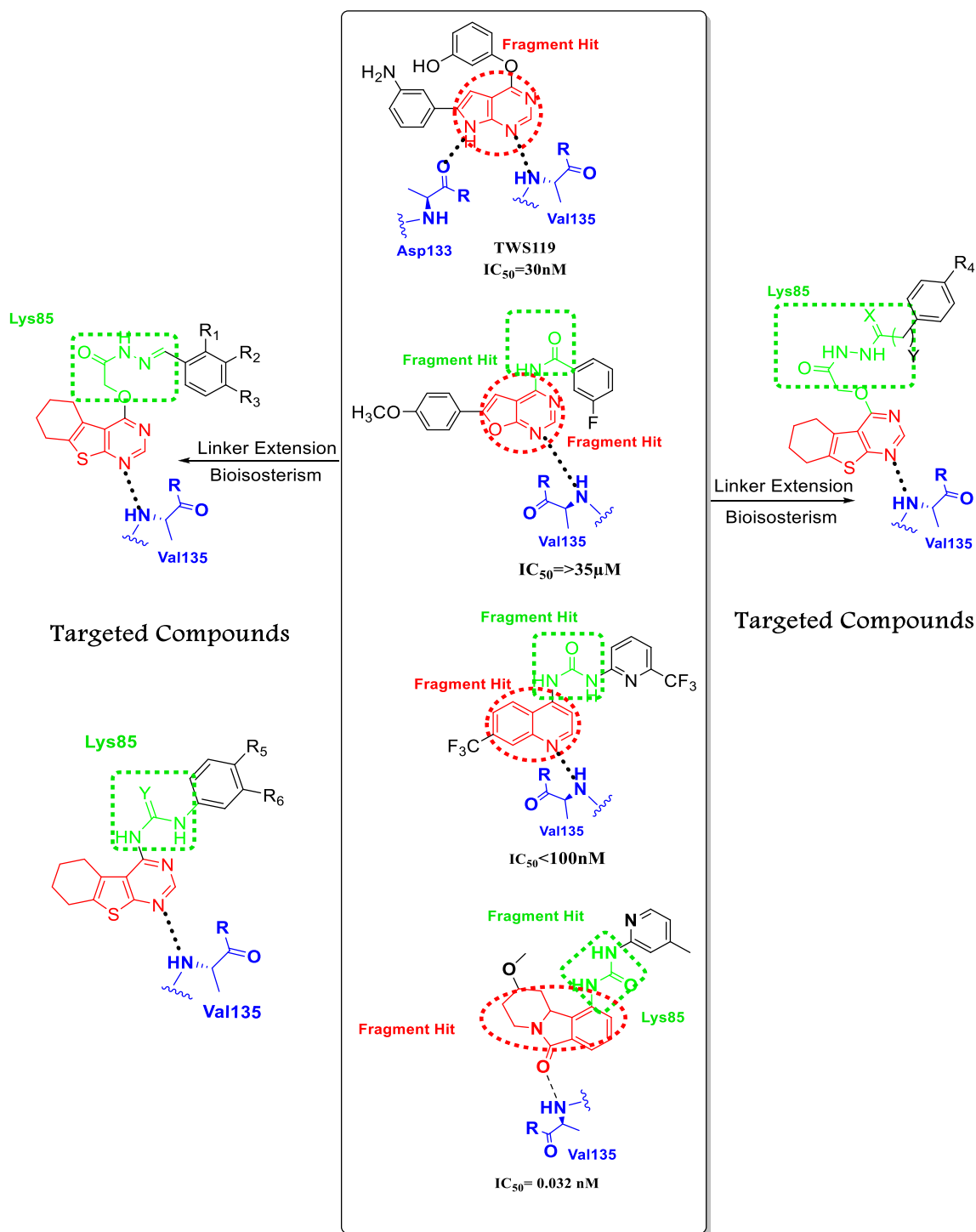
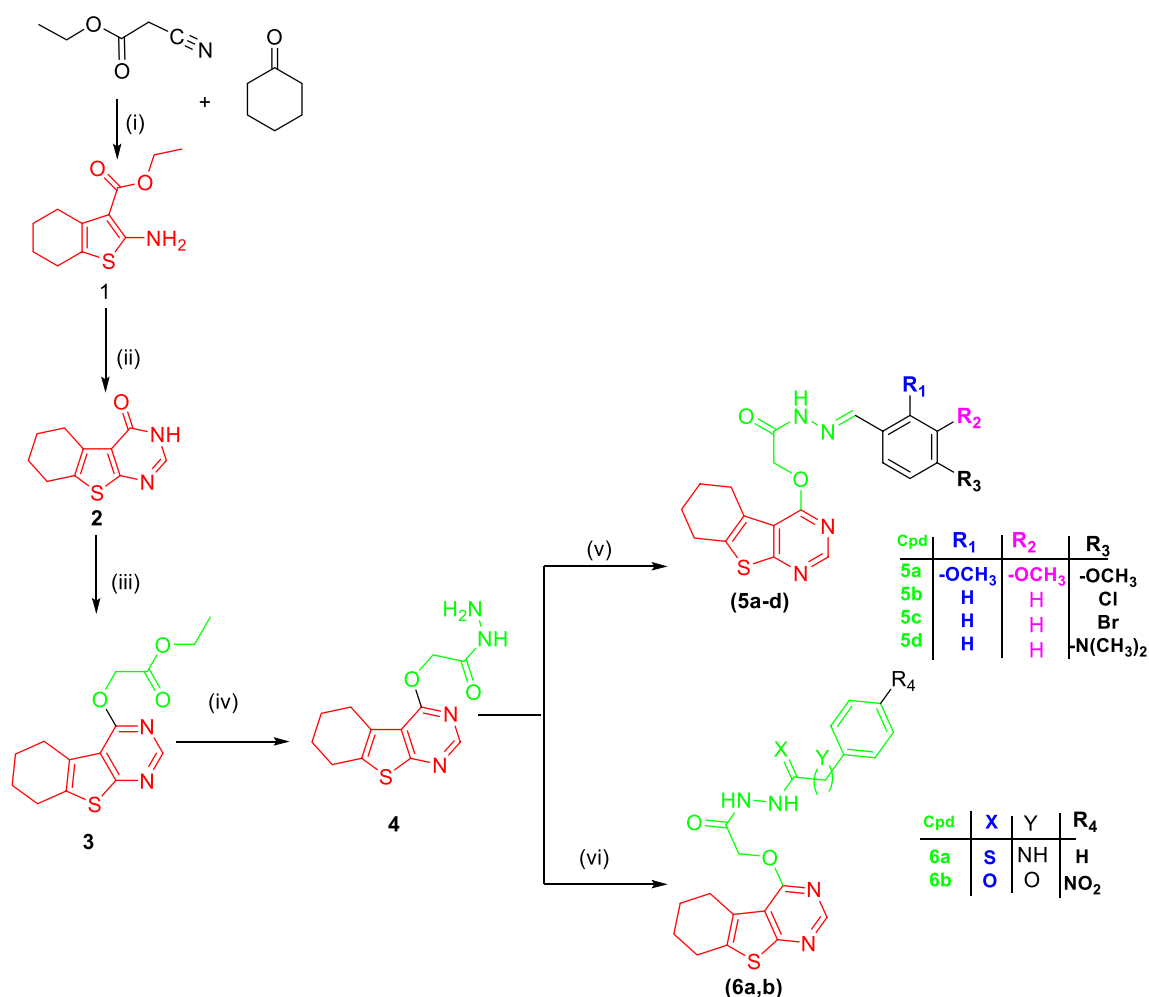


Fig. 2 Schematic representation of targeted compounds

synthesized in following the below-mentioned techniques, were used to obtain final compounds containing a substituted urea moiety. Gewald reaction was used to synthesize ethyl 2-amino-4,5,6,7-tetrahydrobenzo[b]thienopyrimidine

(1) which undergoes the typical Niementowski reaction to get 5,6,7,8-tetrahydrobenzo[4,5]thieno[2,3-d] pyrimidin-4(3H)-one (2) which reacts with ClCH₂COOC₂H₅ in DMF at 80 °C for 24 h in the presence of Cs₂CO₃ to yield ester

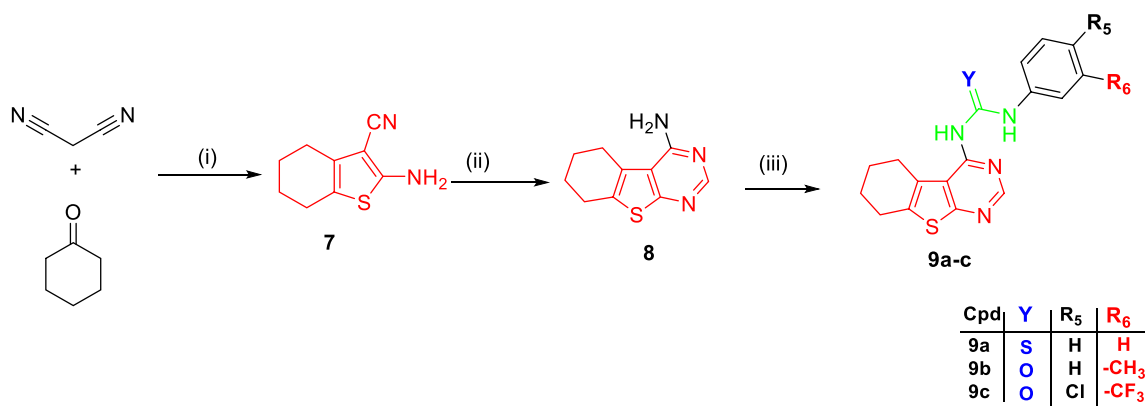


Scheme 1 Reagent and conditions: (i) S¹⁸, piperidine, EtOH, RT, overnight (ii) HCONH₂, reflux, 6 h. (iii) ClCH₂COOC₂H₅, CS₂/CO₂, DMF, 80 °C, 24 h (iv) NH₂NH₂·H₂O, CH₃OH, 0 °C, 4.5 h; (v) Ph-CHO derivatives, gl. AcOH, EtOH, reflux, 24–72 h (vi) *p*-NO₂-Ph-COCl, TEA, dry toluene, reflux, 3 h or PhSCN, TEA, dry toluene, reflux, 48 h

intermediates (3) [17–19]. Thienopyrimidine acetohydrazide (4) is synthesized by hydrazinolysis of ester derivative (3) [20]. Final compounds (5a–d) were synthesized by reacting thienopyrimidine acetohydrazide intermediate (4) with different substituted aldehydes in absolute EtOH and the catalytic quantity of gl. AcOH under reflux for 24–72 h to give the targeted compounds (5a–d) in poor yield % [21]. On the other hand, compounds (6a–b) were obtained by the reaction of thienopyrimidine acetohydrazide intermediate (4) with *p*-nitrobenzoyl chloride for 3 h [22] or phenyl isothiocyanate in dry toluene and catalytic amount of TEA under reflux for 48 h [23]. Preparation of the urea derivatives (9a–c) was achieved through Gewald reaction using malononitrile to afford intermediate (7) which was reacted with formamide to produce 4-aminothienopyrimidine intermediate (8). The previous intermediate reacts with

different phenyl isocyanate or phenyl isothiocyanate to furnish urea derivatives (9a–c) (Scheme 2).

Several analytical and spectral approaches were used to understand the structural properties of the synthesized molecules. The ¹HNMR spectra for the targeted compounds (5a–d, 6a, b and 9a–c) were consistent with total number of protons. ¹HNMR spectra of compounds (5a–d) demonstrated two characteristic signals of the D₂O exchangeable protons of NH groups around δ 11.48–11.94 ppm confirming the *E/Z* configuration. In the ¹HNMR spectra of *E/Z* mixture, a peak at δ 7.92–8.39 ppm represented for N=CH as in compounds (5a–d) confirming the *E/Z* configuration with (3:1) ratio, where vinylic protons of (5a–d) appear at 8.39, 8.22, 8.21 and 8.07 ppm for the *Z*-isomer, whereas they appear at 8.24, 8.05, 8.04 and 7.92 ppm for the *E*-isomer. Intramolecular H-bonding between vinylic proton and the CO–NH



Scheme 2 Reagent and conditions: (i) S¹⁸, TEA, EtOH, RT, overnight (ii) HCONH₂, reflux, 5 h (iii) PhSCN/ PhCNO derivatives, CH₃CN, reflux, 24–48 h

proton leads to a downfield shift in all the vinylic protons in the Z-isomer and an upfield shift in the vinylic protons in the E-isomer. Additionally, the spectra showed one signal of O-CH₂ showed as singlet around δ 5.19–4.70 ppm as in compound (5a–d) confirming the E/Z configuration. Additional protons were shown as a three singlet peaks around δ 3.85, 3.84 and 3.78 ppm of methoxy groups in compound (5a), also, singlet peak around δ 2.97 ppm for two methyl groups of -N(CH₃)₂ as in compound (5d). Furthermore, the extra signal of aromatic protons are around δ 6.75–7.77 ppm.

Regarding compound (6a) showed three signals around δ 10.62–9.34 ppm representing the D₂O exchangeable proton of 3NH group while two signals around 10.93–10.64 ppm representing the D₂O exchangeable proton of 2NH group in compound (6b). Additional aliphatic protons were shown in compounds (6a, b) as singlet peak around δ 4.73 and 4.82 ppm of the O-CH₂ group. Also, the extra signal of aromatic protons are around δ 7.18–8.10 ppm.

On the other hand, ¹HNMR spectra of compounds (9a–c) revealed the appearance of the 2 characteristic signals of D₂O exchangeable protons of NH groups around δ 11.23 and 8.72 ppm. Regarding compounds (9b) spectra, showed singlet peaks at δ 3.06–2.27 ppm, respectively representing for the CH₃ groups. In addition to the signal of aromatic protons are around δ 6.15–7.40 ppm.

In all synthesized compounds, protons were shown as a singlet peak at around δ 1.75–1.79 ppm of four protons at C₆, C₇ of cyclohexyl moiety, a singlet peak at around δ 2.74–2.78 ppm for two protons at C₅ of cyclohexyl moiety, a singlet peak at δ around 2.80–2.88 ppm for two protons at C₈ of cyclohexyl moiety. All spectra showed singlet peak of pyrimidine ring appear at around δ 8.34–8.29 ppm,

The ¹³CNMR spectra were consistent with number of carbons of the targeted compounds (6a, 6b, 9a, 9b), where

shown as a singlet peak at around δ 22.18, 22.84, 25.00, 25.76 (cyclohexyl), 167.18 ppm (C=O) for (6a), two C=O signals at 164.26 and 166.64 ppm for compound (6b). Both compounds (6a, b) showed a signal around δ 48.03–46.93 (OCH₂). IR data stretching signal revealed of N–H group around 3371–3433 cm⁻¹, aromatic C–H around 3000–3070 cm⁻¹, aliphatic C–H at 2908–2989 cm⁻¹, C=O or C=S around 1647–1708 cm⁻¹ and C=N around 1600 cm⁻¹. Mass analysis was performed on compounds showed the presence of M⁺, M⁺+1 and M⁺+2 peaks with A 3:1 relative intensity ratio refers to chlorine isotopes as compounds (5b and 9c) while compound (5c) has relative intensity 1:1 corresponding to bromine isotopes. The founded molecular weights of the titled compounds were compared to their calculated molecular weights (Additional file 1: Sect. "Introduction".)

Biological evaluation

GSK-3 β serine/threonine kinase inhibitory activity in vitro

Preliminary screening at 100 μ M (single dose Concentration) The GSK-3 β tyrosine kinase tests were carried out at Thermo Fischer Scientific USA (www.thermofischer.com/selectscreen). The investigation was carried out to evaluate the GSK-3 β inhibitory activity of the synthesized compounds. During the main reaction of the kinase, a single residue of serine, threonine, or tyrosine in a produced FRET-peptide receives gamma-phosphate of ATP through the biological test Z'-LYTE. In the secondary process, Non-phosphorylated FRET-peptides are identified and degraded by a site-specific protease. The phosphorylation of FRET-peptides inhibits the development reagent from cleaving them. FRET between the donor (coumarin) and acceptor (fluorescein) fluorophores on the FRET-peptide is disrupted by cleavage, while FRET is maintained by uncleaved, phosphorylated FRET-peptides. The percentage of enzymatic activity that the tested substances inhibited GSK-3 β kinase was compared to a 100 μ M as refer-

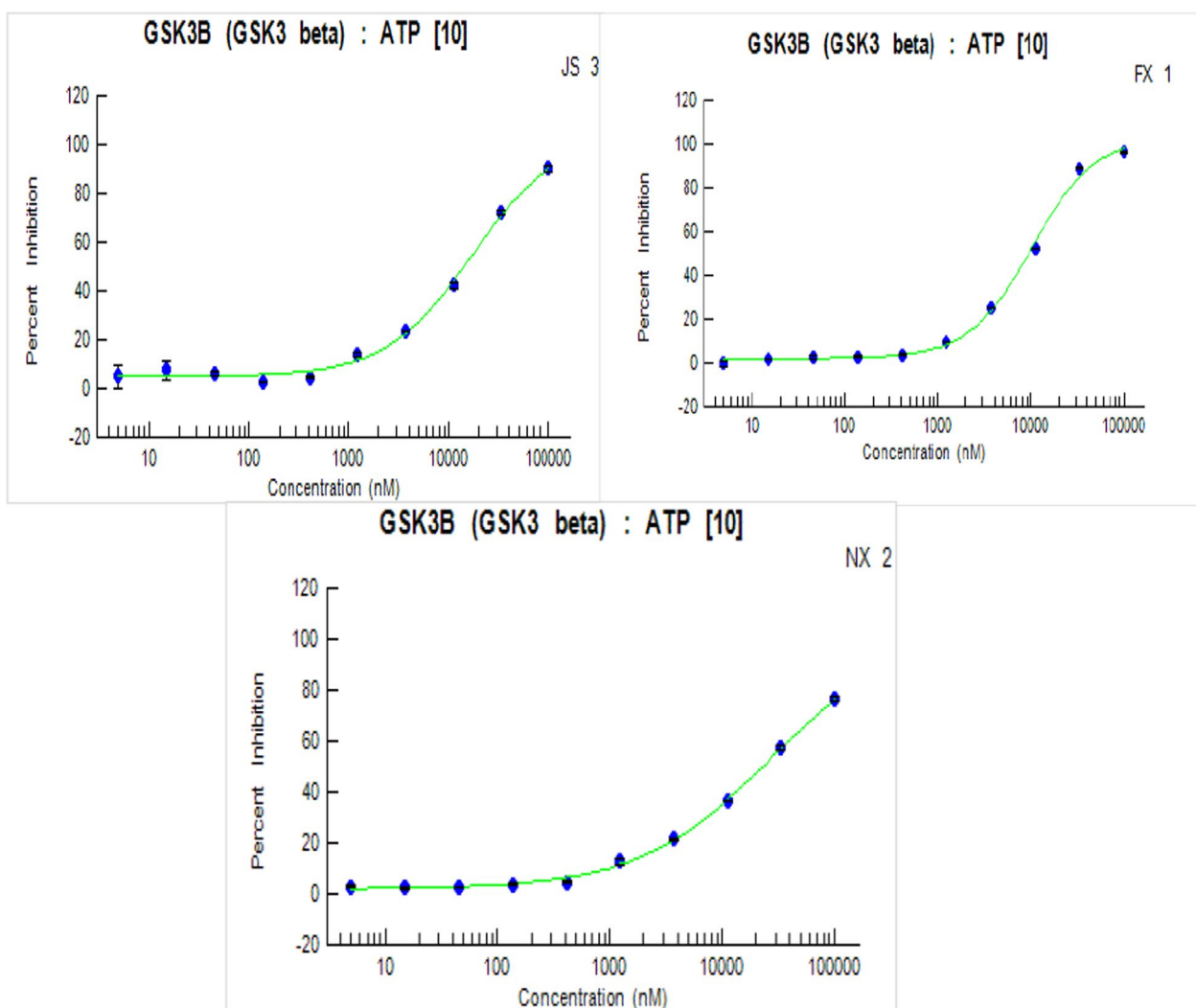


Fig. 3 The target compounds' inhibitory concentration (IC₅₀) on GSK-3 kinase activity

screen employs 60 different Leukemia, melanoma, and additional tumor cell lines of the human from brain, kidney, lung, ovary, colon, breast, and prostate cancers. All compounds were picked based on their NCI codes. NSC: D-820696/1, NSC: D-820697/1, NSC: D-820698/1, NSC: D-820699/1, NSC: D-820700/1, NSC: D-820701/1. The initial 10 μ M one dose percent inhibition assay was performed on the entire NCI 60 cell panel to examine the different chemotypes of this work. The results are presented as a percentage of cell growth on each of the 60 NCI cell line panels for each of the investigated substances in Table 2.

Results of in vitro NCI 60 cell panel assay

On the entire NCI 60 cell panel, an initial in vitro one dose anticancer investigation was performed. The results

for each compound were presented as a mean graph of the percentage growth of the treated cells compared to the untreated control cells. The mean graph of **5d** and **6a** results of the NCI 60 cell line screening program are shown in (Additional file 1: Section 2).

In the thieno[2,3-*d*]pyrimidine derivatives linked to the amide moiety (**5d**), and acyl hydrazide moiety as (**6a**) showed good anti-proliferative activity against specific renal cancer cell line (A498) with 48.37% and 46.98%, respectively (Table 2).

Only acyl hydrazide derivatives (**6b**) and (**6a**) showed moderate inhibitory activity on GSK-3 β kinase with IC₅₀s of 10.2 and 17.3 μ M, respectively, these compounds may be a gloss of hope to develop more selective GSK-3 β inhibitors in the future perspective.

Table 2 Cell growth inhibition % of NCI 60 cancer cell lines displayed by studied final compounds (**5a**, **5b**, **5c**, **5d**, **6a**, **6b**)

Cell line	Percent inhibition of tested compounds					
	5a	5b	5c	5d	6a	6b
Leukemia						
CCRF-CEM	-1.41	-9.27	-6.6	-3.06	-9.95	-4.24
<i>HL-60(TB)</i>	-15.59	-20.1	-6.21	-6.52	-26.88	-12.13
<i>K-562</i>	7.93	0.32	13.48	-1.1	7.06	6.45
<i>MOLT-4</i>	-2.51	-3.88	9.38	0.81	-8.69	-5.68
<i>RPMI-8226</i>	-2.02	2.71	-4.46	-1.59	3.86	3.54
<i>SR</i>	2.15	1.63	8.29	-2.14	-3.94	-8.18
Non-Small Cell Lung Cancer						
<i>A549/ ATCC</i>	-7.39	4.36	1.87	1.15	-2.88	0.86
<i>EKVX</i>	-2.52	3.11	3.66	-0.83	-1.87	-2.61
<i>HOP-62</i>	-0.97	-5.2	-7.64	-2.81	-3.51	-5.83
<i>HOP-92</i>	2.18	0.71	-17.11	-12.12	-5.18	-6.04
<i>NCI-H226</i>	0.3	2.81	-2.67	8.81	-5.15	1.61
<i>NCI-H23</i>	-3.2	-3.09	0.25	-7.75	3.1	-3.5
<i>NCI-H322M</i>	-2.38	0.39	-5.25	3.69	0.95	-2.3
<i>NCI-H460</i>	-4.72	-6.83	-7.79	1.04	-9.19	-11.91
<i>NCI-H522</i>	5.39	-7.4	10.29	4.74	5.09	7.64
Colon Cancer						
<i>COLO 205</i>	-13.34	-15.65	-16.87	-19.33	-14.84	-17.8
<i>HCT-116</i>	-2.14	-1.09	3.24	-3.26	1.5	-2.14
<i>HCT-15</i>	-1.3	-3.67	-2.27	-3.18	0.17	3.44
<i>HT29</i>	-2.84	-10.73	-3.17	-5.43	-7.67	-2.8
<i>KM12</i>	-4.43	-3.25	-2.83	-4.72	-5.57	-2.31
<i>SW-620</i>	-0.67	-2.86	-2.19	2.39	-2.97	-0.18
CNS Cancer						
<i>SF-268</i>	0.3	4.27	5.08	1.44	-1.63	-1.73
<i>SF-295</i>	0.79	-0.79	-0.63	-2.1	2.64	-2.08
<i>SF-539</i>	5.93	-1.8	1.02	-4.86	2.42	2.53
<i>SNB-19</i>	6.88	9.77	5.53	3.31	5.27	9.18
<i>SNB-75</i>	28.47	18.43	13.6	18.79	14.57	20.29
<i>U251</i>	0.3	15.94	6.99	-1.33	3.33	5.59
Melanoma						
<i>LOX IMVI</i>	4.82	7.09	3.68	2.93	1.31	4.71
<i>MALME-3 M</i>	2.96	6.05	-6.85	-6.83	-5.31	3.05
<i>M14</i>	1.68	2	-0.52	-5.42	0.96	0.05
<i>MDA-MB-435</i>	-3.78	-4.44	0.85	-1.25	-2.38	-2.51
<i>SK-MEL-2</i>	-5.72	-9.81	-2.58	-3.47	-17.39	-5.07
<i>SK-MEL-28</i>	-3.83	-2.26	-8.66	-1.38	-5.56	-0.83
<i>SK-MEL-5</i>	1.37	-4.02	-0.82	0.27	-1.1	0.34
<i>UACC-257</i>	-16.53	-5.53	-3.03	-4.34	-5.37	-4.29
<i>UACC-62</i>	8.06	4.84	6.58	5.34	7.2	0.88
Ovarian Cancer						
<i>IGROV1</i>	1.47	11.04	2.52	14.45	-2.19	1.22
<i>OVCAR-3</i>	-10.52	-16.96	-7.55	-4.24	-11.84	-12.61
<i>OVCAR-4</i>	-1.36	-7.63	-8.18	-7.86	-8.59	-4.28
<i>OVCAR-5</i>	5	8.96	10.01	8.97	3.88	0.17
<i>OVCAR-8</i>	-9.71	-3.32	-4.36	-4.59	-1.94	-2.71
<i>NCI/ADR-RES</i>	-9.83	-4.28	-6.04	-7.97	-1.67	-3.67

Table 2 (continued)

Cell line	Percent inhibition of tested compounds					
	5a	5b	5c	5d	6a	6b
SK-OV-3	-16.24	-5.64	-13.54	-20.61	-6.24	-12.83
Renal Cancer						
786-0	0.81	2.11	5.22	-7.8	1.23	0.04
A498	11.84	11.06	21.32	48.37	46.98	-0.23
ACHN	0.55	-2.86	-5.34	-2.45	-3.69	-2.45
CAKI-1	7.04	4.53	16.68	5.26	1.14	5.18
RXF 393	-9.95	4.13	-7.61	7.97	-8.94	-11.79
SN12C	5.91	2.55	3.09	-0.68	3.79	2.5
TK-10	-20.81	-20.06	-11.04	-19.44	-15.71	-12.29
UO-31	23.31	23.08	16.55	23.98	14.76	21.12
Prostate Cancer						
PC-3	2.52	3.8	-12.53	3.93	3.65	-1.65
DU-145	-5.76	-6.67	-0.13	-4.77	-8.64	-5.56
Breast Cancer						
MCF7	10.68	11.7	8.67	7.82	12.27	8.21
MDA-MB-231/ATCC	6.61	7.6	11.25	-1.8	3.71	-2.07
HS 578 T	7.21	7.62	7.31	5.71	-6.34	-2.09
BT-549	-1.41	-5.46	2.58	-9.47	-2.68	-0.91
T-47D	4.24	6.96	-0.52	0.95	6.64	1.13
MDA-MB-468	-13.63	-8.56	-14.65	15.75	-14.73	-5.3

● 40–50% inhibition of growth, ● 50–60% inhibition of growth, ● 60–70% inhibition of growth, ● 70–80% inhibition of growth, ● 80–100% inhibition of growth

Molecular docking

In order to better understand the binding modalities and directions of active compounds into binding site of ATP for GSK-3 β kinase enzyme, docking procedure is carried out using MOE software version 2019, and one of the ten retrievable docking configurations was picked. GSK-3 β crystal structure in interaction with lead compound (**IV**) was obtained (PDB code: **1J1B**).

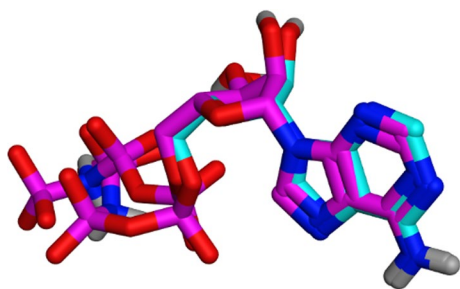


Fig. 4 The aligning of the lead compound's X-ray active conformer (coloured in cyan) with the redocked posture (purple) at the GSK-3 β binding site

The binding modes of GSK-3 β inhibitors showed that they interact with the ATP binding site via hydrogen bonding with Asp133 or Val135 which represent two out of the three interactions in all inhibitors namely: two hydrogen bond donors interaction with the backbone carbonyls of Val135 and Asp133, and one hydrogen bond acceptor interacts with Val 135's -NH. The ligands also interact hydrophobically with Ile62, Phe67, Leu188, and Cys199 side chains, as well as polarly with Thr138, Glu185, and Asp200.

Validation of docking protocol

Redocking phosphoaminophosphonic acid-adenylate ester (ANP) was used to validate the docking algorithm into the active site of GSK-3 β . With a root mean square difference (RMSD) of 1.83 Å between the top docking pose and the original crystallographic ligand, this was found to be effective in retrieving the previously described X-ray crystal structure binding site of ligand (Fig. 4).

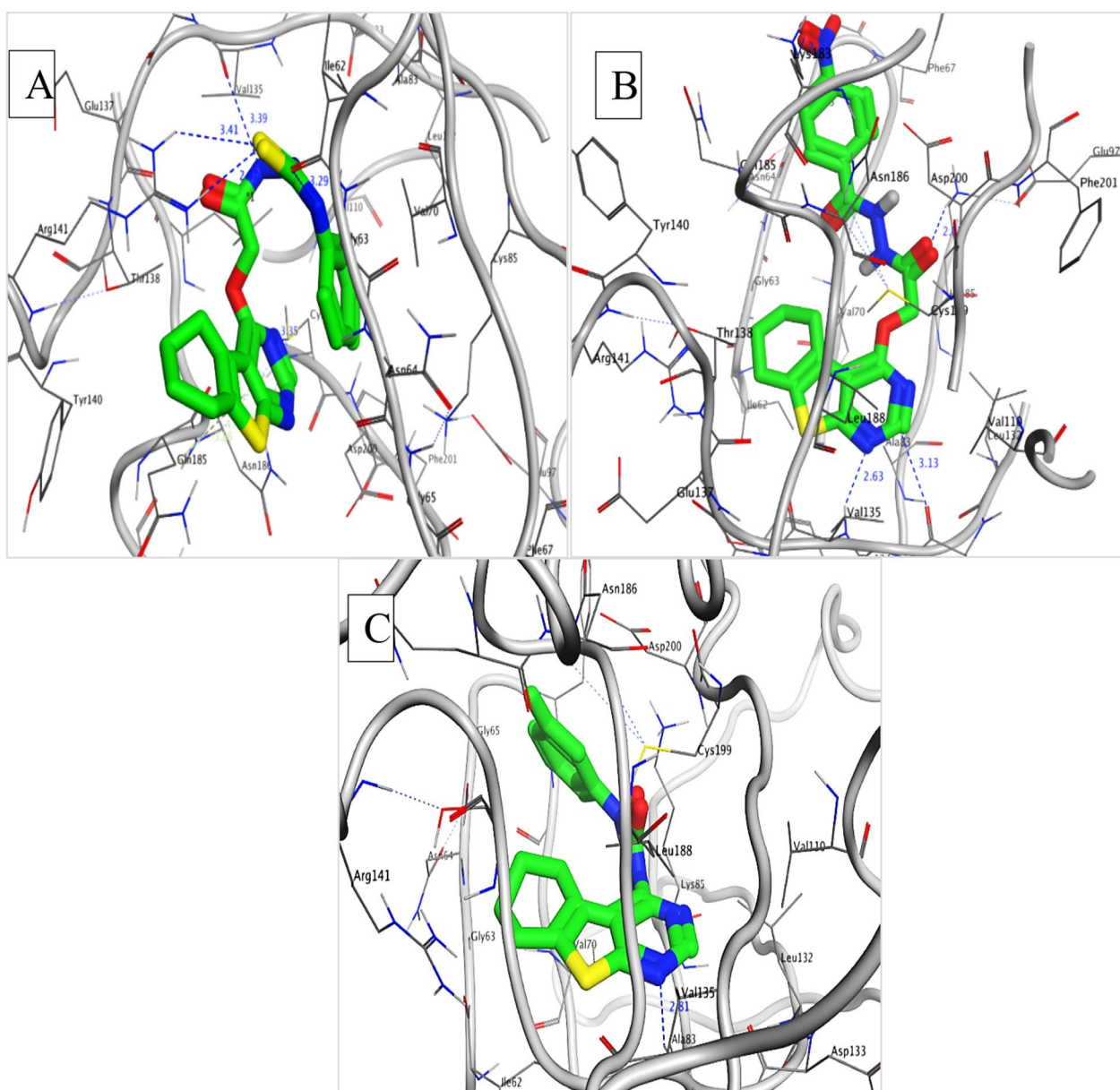


Fig. 5 Targeted compounds bind with GSK-3 β binding site (PDB ID: 1J1B). Compound **6a** in ATP binding site of GSK-3 β showing four hydrogen bond interactions with Val135, Arg141, Ile62, Cys 199 residues, and hydrophobic interaction with Gln185 while compound **6b** identified a critical hydrogen bond and its distances from the GSK-3 β binding site; makes hydrogen bond interaction with Val135, Asp133, Lys85, Lys183 residues, and hydrophobic interaction with Val70 and Docking pose of compound **9b** show the same critical interactions with the GSK-3 β binding site; hydrogen bond interaction with Val135 residue and hydrophobic interaction with Val70. (Dotted blue lines are represent for hydrogen bonds and pale green bold line for hydrophobic interaction)

Binding mode of the targeted compounds with GSK-3 β binding site (PDB ID: 1J1B)

See Fig. 5.

In silico predictive ADMET study

The pharmacodynamic properties of the synthesized compounds were studied in silico for the prediction of

their possible transport to the site of action. Also, due to the importance of their molecular characteristics for human pharmacokinetics, molecular properties of new drugs were examined throughout development. For example, Lipinski's rule of five determines if a molecule of interest possesses chemical and physical qualities that would make it likely to be active orally. Oral bioavailability is likely to happen if at least three of the

following requirements were met: There are a maximum of 5 H-bond donors, a maximum molecular weight of 500 Da, a maximum log P of 5, a maximum number of violations of 1 and a maximum number of H-bond acceptors of 10. The quantity of rotatable bonds, polar surface area, and drug oral bioavailability are all strongly correlated. According to the Veber rule, oral bioavailability for compounds with less than 10 rotatable bonds and a polar surface area (PSA) > 140 Å² is acceptable. Additionally, ADME was determined using the SWISSADME program. Additionally, the SWISSADME made a prediction regarding the potential pharmacokinetic effects on a number of cytochromes P450 enzymes (CYP450), including CYP1A2, CYP2C19, CYP2C9, CYP2D6, and CYP3A4, as well as the likelihood that these enzymes will serve as substrates (inducers) of Permeability glycoprotein (P-gp) (Table 3). **Boiled-egg plot chart**

ADMET-Graphic, a 2D plot created utilizing determined by Swiss ADME, is used to display the findings of the ADMET study. All the substances were plotted outside the in yellow circle that Blood Brain Barrier (BBB) and Human Intestinal Absorption (HIA) graphs some compounds are in white circle and 3 compound are outside (Fig. 6).

Pharmacokinetic analyses of compounds (5a-d, 6a, b and 9a-c) on cytochrome P450 enzymes and P-glycoprotein revealed that CYP3A4 is predicted to be inhibited by all compounds, and all compounds except compound (6b) are predicted to be inhibitors of CYP2C9 & CYP2C19, while CYP1D6 is predicted to be inhibited by compounds (5a, 5d, 6a, 9a and 9b) and all compounds, with the exception of those (5a, 5d and 6b), are inhibitors of CYP1A2. Regarding P-gp, all substances are impermeable to glycoprotein except for (9a-9b). Additionally, the blood-brain barrier (BBB) is predicted to not be pass by all of the compound so it is expected to have no side effect on brain.

Conclusion

This work involved the design and synthesis of new GSK-3β inhibitors containing urea /acetyl hydrazide coupled thienopyrimidine inhibitors. The synthesized compounds were examined for their in vitro GSK-3β inhibitory activities. Compounds 6a, 6b, 9a, 9b and 9c were found to be moderately active as GSK-3β inhibitors with IC₅₀ range (10.2–41.8 μM). In addition, six of the final compounds (5a, 5b, 5c, 5d, 6a and 6b). The National Cancer Institute "NCI" chose them for a single dose screening programmed at 10 μM in the whole NCI 60 cell panel. The thienopyrimidine-based derivative

Table 3 Predicted AMDE and pharmacological parameters for targeted compounds (5a-d, 6a-b, 9a-c)

Comp	M.wt (g/mol)	H. bond Donor	H. bond acceptor	Log p	TPSA	Lipinski violation	Rotatable bonds
5a	456.51	1	8	3.42	132.40 Å ²	0	9
5b	400.88	1	5	4.01	104.71 Å ²	0	6
5c	445.33	1	5	4.11	104.71 Å ²	0	6
5d	409.50	1	5	3.56	107.95 Å ²	0	7
6a	413.52	3	4	3.31	148.50 Å ²	1	8
6b	427.43	2	7	2.21	167.27 Å ²	1	8
9a	340.47	2	2	3.88	110.17 Å ²	0	4
9b	338.43	2	3	3.67	95.15 Å ²	0	4
9c	426.84	2	6	4.92	95.15 Å ²		5
Comp	CYP1A2 inhibitor	CYP2C19 inhibitor	CYP2C9 inhibitor	CYP2D6 inhibitor	CYP3A4 inhibitor	P-gp substrate	BBB permeant
5a	NO	YES	YES	YES	YES	NO	NO
5b	YES	YES	YES	NO	YES	NO	NO
5c	YES	YES	YES	NO	YES	NO	NO
5d	NO	YES	YES	YES	YES	NO	NO
6a	YES	YES	YES	YES	YES	NO	NO
6b	NO	NO	NO	NO	YES	NO	NO
9a	YES	YES	YES	YES	YES	YES	NO
9b	YES	YES	YES	NO	YES	YES	NO
9c	YES	YES	YES	NO	YES	NO	NO

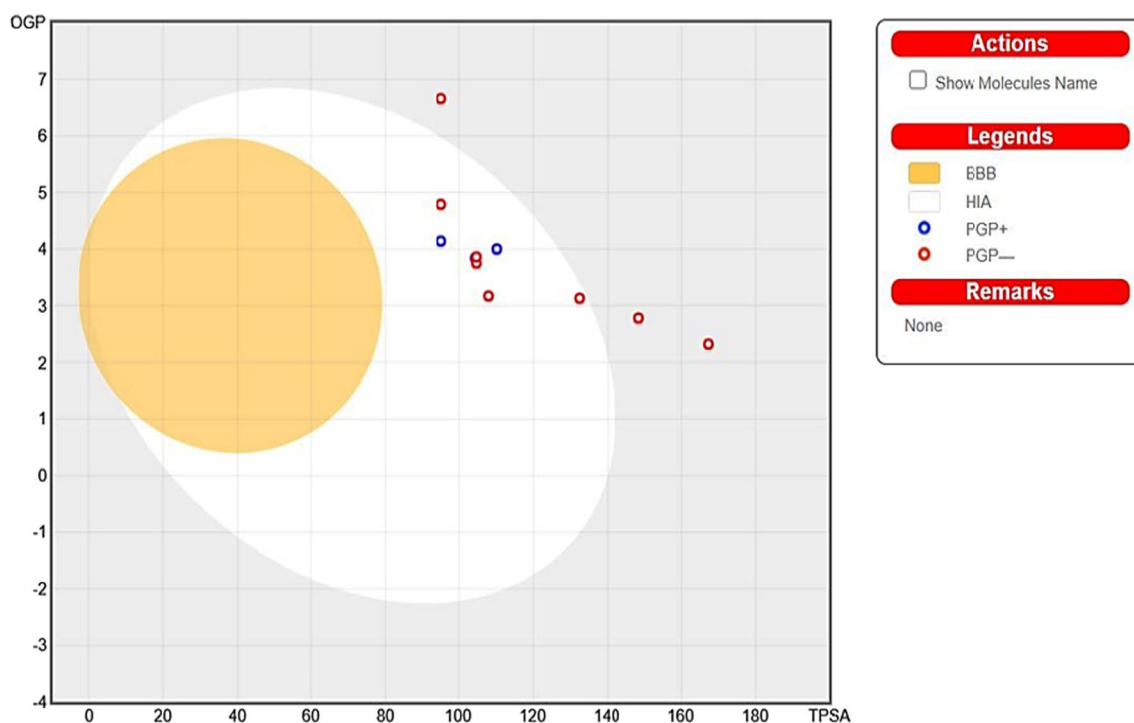


Fig. 6 The newly synthesized compounds' Blood Brain Barrier (BBB) plot and human intestinal absorption (HIA)

(5d and 6a) showed good anti-proliferative activity against specific cell lines as renal cancer cell line. Finally, molecular docking study was performed to predict how these compounds bind to the GSK-3 β active site. Compounds (6a, 6b, 9b) showed similar orientation and binding interactions with a larger likelihood to enter the GSK-3 β pocket. The study of computer aided ADMET was also carried out, using Swiss ADME to investigate the pharmacokinetic properties of the tested compounds.

Experimental Chemistry

Loba chemie and alfa-aesar organics provided the starting ingredients and reagents, which were employed without further purification. Fisher Scientific or Sigma-Aldrich solvents were obtained and used without further purification. Drying of the solvent were done using molecular Sieves. TLC was used to monitor chemical reactions using silica gel 60 F254 packed on aluminium sheets purchased from Merck and viewed under ultraviolet light ($\lambda = 254$ nm). Silica (240–70 mm) was used for column chromatography. Stuart Scientific gear was used to determine melting points and were uncorrected. NMR spectra were

acquired on a Bruker at 400 MHz for ^1H NMR and at 100 MHz for ^{13}C NMR in ppm scale. Chemical shifts (δH) were provided relative to DMSO- d_6 . All coupling constant (J) values were given in Hz. The acronyms are as follows: s: singlet; d: doublet; and m: multiplet. IR spectra were recorded on Shimadzu FT-IR 8400S spectrophotometer. An EI-MS LC/Ms/Ms mass spectrometer API 200 (AB Sciex Instrument) was utilized to get EI-MS spectra. Also, elemental analyses were also performed.

Ethyl 2-amino-4,5,6,7-tetrahydrobenzo[b]thiophene-3-carboxylate (1)

To a stirred solution of cyclohexanone (5.2 g, 53 mmol) in ethanol (15 mL), were added ethyl cyanoacetate (6.37 g, 57 mmol), sulfur powder (1.60 g, 50 mmol) and piperidine (1.3 g, 15 mmol) and the resulting reaction mixture was stirred at either 50 °C overnight in water bath. The progress of reaction was monitored by TLC, after completion of disappearance of starting materials, cooled the reaction mixture to ambient temperature and the resulting solids were filtered and dried under vacuum. The obtained crude solid was further purified by recrystallization by ethanol to afford desired compound-1 (9.76 g, yield: 80.1%) as a yellow crystal [24].

5,6,7,8-Tetrahydrobenzo [4,5] thieno[2,3-d] pyrimidin-4(3H)-one (2)

A solution of **1** (1 g, 4.4 mmol) in formamide (10 mL, 11.3 g, 250 mmol) was heated under reflux for 13 h. After cooling, the resulting solid precipitate was collected by filtration and recrystallized from ethanol to afford the titled compound-2 (**0.72 g, yield: 78.6%**) as gray crystals [25].

Ethyl 2-((5,6,7,8-tetrahydrobenzo [4,5] thieno[2,3-d] pyrimidin-4-yl) oxy) acetate (3)

An equimolar mixture of 4,5,6,7-tetrahydrobenzo[b] thieno[2,3-d] pyrimidin-4(3H)-one (2) (6.18 g, 30 mmol), ethyl chloroacetate (3 mL, 30 mmol) and excess Cs₂CO₃ (6.5 g, 0.02 mol) in 30 mL of DMF was refluxed for 24 h. Most of the solvent was evaporated, and the reaction mixture was then poured onto ice water to give a solid product. Crystallization of the crude product from light petroleum (60–80 °C) yielded the title product **3** (**5.24 gm, yield: 64.1%**) as white crystals [26].

2-((5,6,7,8-Tetrahydrobenzo [4,5] thieno[2,3-d] pyrimidin-4-yl) oxy) acetohydrazide (4)

A mixture of **3** (2.92 g, 10 mmol) and hydrazine hydrate (0.5 ml, 10 mmol) in methanol (60 mL) was heated under reflux for 4.5 h, left to cool. The formed precipitate was filtered, dried, and then recrystallized from ethanol to afford **4** (**1.61 gm, yield: 61.1%**) as Pale-yellow crystals [26].

Synthesis of targeted compounds (5a-d)

General procedure

The hydrazide (**4**) (2.78 g, 10 mmol) and the appropriate aromatic aldehyde, namely 2,3,4 trimethoxybenzaldehyde, *p*-chlorobenzaldehyde, *p*-bromobenzaldehyde, and dimethylaminobenzaldehyde (10 mmol), in ethanol (30 mL) and drops of acetic acid were heated under reflux for 48–72 h. A solid product was precipitated during reflux, which was filtered, washed well, dried and then recrystallized from a suitable solvent to afford **5a–d** (**yield: 61–64%**) (Spectral data in Supplementary Material).

2-((5,6,7,8-Tetrahydrobenzo [4,5] thieno[2,3-d] pyrimidin-4-yl) oxy)-*N'*-(2,3,4-trimethoxybenzylidene) acetohydrazide (**5a**) White powder, m.p 280–281 °C; yield: 61% (R_F=0.64, Elution system: 1 ml of methylene chloride: 0.2 ml methanol: 0.4 ml hexane); ¹HNMR (400 MHz, DMSO-*d*₆) δ 11.79, 11.64 (2s, 1H, NH D₂O exchangeable, *Z* & *E* confirmations), 8.30 (s, 1H, pyrimidine H), 8.39, 8.24 (2s, 1H, CH=N, *Z* & *E* confirmations (ratio 1:3)), 7.60, 7.55 (2d, *J*=8.9 Hz, 8.8 Hz, 1H, ArH, *Z* & *E* confirmations), 6.92

(d, *J*=8.0 Hz, 1H, ArH), 5.16, 4.71 (2s, 2H, CH₂-O, *Z* & *E* confirmations), 3.84 (s, 3H, -OCH₃), 3.85 (s, 3H, -OCH₃), 3.78 (s, 3H, -OCH₃), 2.86 (s, 2H, cyclohexyl), 2.78 (s, 2H, cyclohexyl), 1.79 (s, 4H, cyclohexyl); FT-IR (ν_{max}, cm⁻¹): 3425 (NH), 3062 (aromatic CH), 2939 (aliphatic CH), 1681 (C=O); MS (Mwt.: 456): *m/z*, 456.60 [M⁺, (45.55%)], 280.48 (100%); Anal. Calcd for C₂₂H₂₄N₄O₅S: C, 57.88; H, 5.30; N, 12.27; Found: C, 58.12; H, 5.47; N, 12.50.

N'-(4-Chlorobenzylidene)-2-((5,6,7,8-tetrahydrobenzo [4,5] thieno[2,3-d] pyrimidin-4-yl) oxy) acetohydrazide (**5b**) White powder, m.p 275–276 °C; yield: 64%, (R_F=0.68, Elution system: 1 ml of methylene chloride: 0.2 ml methanol: 0.4 ml hexane); ¹HNMR (400 MHz, DMSO-*d*₆) δ 11.94, 11.84 (2s, 1H, NH, D₂O exchangeable, *Z* & *E* confirmations), 8.30 (s, 1H, pyrimidine H), 8.22, 8.05 (2s, 1H, CH=N, *Z* & *E* confirmations (ratio 1:3)), 7.77 (d, *J*=8.8 Hz, 2H, ArH), 7.52 (d, *J*=8.8 Hz, 2H, ArH), 5.19, 4.74 (2s, 2H, CH₂-O, *Z* & *E* confirmations), 2.86 (s, 2H, cyclohexyl), 2.76 (s, 2H, cyclohexyl), 1.78 (s, 4H, cyclohexyl); FT-IR (ν_{max}, cm⁻¹): 3421 (NH), 3008 (aromatic CH), 2943 (aliphatic CH), 1685 (C=O); MS (Mwt.: 400): *m/z*, 400.41 [M⁺, (38.27%)], 401.85 [M⁺ + 2, (23.55%)], 47.77(100%); Anal. Calcd for C₁₉H₁₇ClN₄O₂S: C, 56.93; H, 4.27; N, 13.98; Found: C, 57.05; H, 4.41; N, 14.19. (Spectral data coincides with reported) [26].

N'-(4-Bromobenzylidene)-2-((5,6,7,8-tetrahydrobenzo[4,5] thieno[2,3-d]pyrimidin-4-yl)oxy)acetohydrazide (**5c**) White powder, m.p 290–292 °C; yield: 62%; (R_F=0.71, Elution system: 1 ml of methylene chloride: 0.2 ml methanol: 0.4 ml hexane); ¹HNMR (400 MHz, DMSO-*d*₆) δ 11.85 (br. s, 1H, NH, D₂O exchangeable), 8.30 (s, 1H, pyrimidine H), 8.21, 8.04 (2s, 1H, CH=N, *Z* & *E* confirmations (ratio 1:3)), 7.67 (m, 4H, ArH), 5.19, 4.74 (2s, 2H, CH₂-O, *Z* & *E* confirmations), 2.86 (s, 2H, cyclohexyl), 2.76 (s, 2H, cyclohexyl), 1.78 (s, 4H, cyclohexyl); FT-IR (ν_{max}, cm⁻¹): 3421 (NH), 3070 (aromatic CH), 2943 (aliphatic CH), 1666 (C=O); MS: (Mwt.: 445): *m/z*, 445.13 [M⁺, (36.68%)], 447.59 [M⁺ + 2, (35.03%)], 81.90 (100%); Anal. Calcd for C₁₉H₁₇BrN₄O₂S: C, 51.24; H, 3.85; N, 12.58; Found: C, 51.41; H, 3.98; N, 12.75.

N'-(4-(Dimethylamino) benzylidene)-2-((5,6,7,8-tetrahydrobenzo [4,5] thieno[2,3-d] pyrimidin-4-yl) oxy) acetohydrazide (**5d**) Pale yellow powder, m.p 285 °C; yield: 64%; (R_F=0.76, Elution system: 1 ml of methylene chloride: 0.2 ml methanol: 0.4 ml hexane); ¹HNMR (400 MHz, DMSO-*d*₆) δ 11.56, 11.48 (2s, 1H, NH, D₂O exchangeable, *Z* & *E* confirmations), 8.30 (s, 1H, pyrimidine H), 8.07, 7.92 (2s, 1H, CH=N, *Z* & *E* confirmations (ratio 1:3)), 7.53 (d, *J*=8.9 Hz, 2H, ArH), 6.75 (d, *J*=9.0 Hz, 2H,

ArH), 5.14, 4.70 (2s, 2H, $\text{CH}_2\text{-O}$, *Z* & *E* confirmations), 2.97 (s, 6H, 2-N- CH_3), 2.86 (s, 2H, cyclohexyl), 2.76 (s, 2H, cyclohexyl), 1.79 (s, 4H, cyclohexyl); **FT-IR** (ν max, cm^{-1}): 3421 (NH), 3066 (aromatic CH), 2908 (aliphatic CH), 1678 (C=O); **MS**: (Mwt.: 409): *m/z*, 409.83 [M^+ , (90.98%)], 139.68 (100%); **Anal.** Calcd for $\text{C}_{21}\text{H}_{23}\text{N}_5\text{O}_2\text{S}$: C, 61.59; H, 5.66; N, 17.10; O, 7.81; S, 7.83; Found: C, 61.38; H, 5.79; N, 17.28.

Synthesis of targeted compounds (6a, b)

A mixture of (4) (0.17 g, 0.63 mmol) with phenyl isothiocyanate (0.17 g, 1.26 mmol) were dissolved in 15 ml dry toluene under reflux for 48 h and follow up the reaction with TLC till end the reaction, then cool to room temperature. A solid product was precipitated which was filtrated, dried to give compound **6a** (yield 64%) as white powder (Spectral data in supplementary material).

A mixture of compound (4) (0.3 g, 1.077 mmol) with 4-nitrobenzoyl chloride (0.2 g 1.077 mmol) was dissolved in 15 ml dry toluene and add drops of TEA in ice bath, stirring for 3 h and follow up the reaction with TLC till end the reaction. A solid product was precipitated during stirring, which was filtered off, washed well, dried and then recrystallized from ethanol to afford **6b** (yield 64%) as yellow powder (Spectral data in supplementary material).

N-Phenyl-2-(2-((5,6,7,8-tetrahydrobenzo [4,5] thieno[2,3-*d*] pyrimidin-4-yl)oxy)acetyl hydrazine-1-carbothioamide (**6a**) White powder, m.p. 270–272 °C; yield: 64%; (R_F =0.81, Elution system: 1 ml of methylene chloride: 0.2 ml methanol: 0.4 ml hexane); $^1\text{H NMR}$ (400 MHz, $\text{DMSO-}d_6$) δ 10.62 (s, 1H, NH, D_2O exchangeable), 9.85 (s, 1H, NH, D_2O exchangeable), 9.34 (s, 1H, NH, D_2O exchangeable), 8.31 (s, 1H, pyrimidine H), 7.56 (d, J =8.0 Hz, 2H, ArH), 7.34 (t, J =8.0 Hz, 2H, ArH), 7.18 (t, J =8.0 Hz, 1H, ArH), 4.73 (s, 2H, O- CH_2), 2.80 (s, 2H, cyclohexyl), 2.76 (s, 2H, cyclohexyl), 1.80 (s, 4H, cyclohexyl). $^{13}\text{C NMR}$ (100 MHz, $\text{DMSO-}d_6$) δ 22.18, 22.84, 25.00, 25.76 (cyclohexyl), 48.03 (CH_2), 122.09, 125.63, 128.59, 131.14, 133.92, 139.34, 148.28, 157.88, 162.49, 167.18 (C=O), 180.88 (C=S); **FT-IR** (ν max, cm^{-1}): 3414, 3329, 3221 (3NH), 3028 (aromatic CH), 2927 (Aliphatic CH), 1670 (C=O); **MS**: (Mwt.: 413): *m/z*, 413.57 [M^+ , (45.19%)], 109.31 (100%); **Anal.** Calcd for $\text{C}_{19}\text{H}_{18}\text{N}_4\text{O}_2\text{S}_2$: C, 55.19; H, 4.63; N, 16.94; Found: C, 55.45; H, 4.72; N, 17.12.

4-Nitro-*N'*-(2-((5,6,7,8-tetrahydrobenzo [4,5] thieno[2,3-*d*] pyrimidin-4-yl) oxy) acetyl benzo hydrazide (**6b**) Yellow powder, m.p. 320–321 °C; yield: 64%; (R_F =0.41, Elution system: 1 ml of methylene chloride: 0.2 ml methanol: 0.4 ml hexane); $^1\text{H NMR}$ (400 MHz, $\text{DMSO-}d_6$) δ 10.93

(s, 1H, NH, D_2O exchangeable), 10.64 (s, 1H NH, D_2O exchangeable), 8.34 (m, 3H, 2ArH, 1H pyrimidine H), 8.10 (d, J =8.8 Hz, 2H, ArH), 4.82 (s, 2H O- CH_2), 2.88 (s, 2H, cyclohexyl), 2.74 (s, 2H, cyclohexyl), 1.75 (s, 4H, cyclohexyl); $^{13}\text{C NMR}$ (100 MHz, $\text{DMSO-}d_6$) δ 22.23, 22.87, 25.00, 25.77 (cyclohexyl), 45.89 (CH_2), 122.10, 124.19, 129.50, 129.71, 131.18, 131.27, 133.55, 138.35, 148.55, 149.87, 157.27, 162.16, 164.26, 166.64 (C=O); **FT-IR** (ν max, cm^{-1}): 3429, 3209 (2NH), 3105 (aromatic CH), 2974 (aliphatic CH), 1716, 1651 (C=O); **MS**: (Mwt.: 427): *m/z*, 427.47 [M^+ , (29.71%)], 142.21 (100%). **Anal.** Calcd for $\text{C}_{19}\text{H}_{17}\text{N}_5\text{O}_5\text{S}$: C, 53.39; H, 4.01; N, 16.38; Found: C, 53.51; H, 4.24; N, 16.59.

Amino-4,5,6,7-tetrahydrobenzo[b]thiophene-3-carbonitrile (7)

A mixture of cyclohexanone (1.85 g, 1.96 mL, 19.0 mmol), malononitrile (1.32 g, 1.25 mL, 57 mmol), sulfur powder (0.64 g, 20.0 mmol) and triethylamine (2.03 g, 2.12 mL, 20 mmol) was heated with ethanol (30 mL) in water bath at 50–60 °C overnight. After cooling, the resulting crystals was collected by filtration to give the titled compound (7) (3.05 g, yield: 89.05%) as buff crystals [27].

5,6,7,8-Tetrahydrobenzo [4,5] thieno[2,3-*d*] pyrimidin-4-amine (8)

A mixture of 2-amino-4,5,6,7-tetrahydrobenzo[b]thiophene-3- carbonitrile (7) (1.78 g, 10.0 mmol) and formamide (3.60 g, 80.0 mmol) was refluxed for 5 h. On cooling, a precipitate crystallized, which was filtered off to produce (8) (1.76 g Yield: 86%) as orange crystals [28].

Phenyl-3-(5,6,7,8-tetrahydrobenzo [4,5] thieno[2,3-*d*] pyrimidin-4-yl) thiourea (9a-c)

General procedure A mixture of compound 8 (0.63 mmol, 0.129 gm) and appropriate phenyl isothiocyanate/ phenyl isocyanate derivative (1.26 mmol) in 10 mL acetonitrile was heated under reflux for 24–48 h. After cooling, the resulting crystals was collected by filtration, dried and recrystallized from ethanol to afford (9a-c) (Yield 80–85%) [29] (Spectral data in supplementary material).

*Phenyl-3-(5,6,7,8-tetrahydrobenzo [4,5] thieno[2,3-*d*] pyrimidin-4-yl) thiourea (9a)* Yellow powder, m.p 300 °C; Yield: 84%, (R_F =0.40, Elution system: 1 mL of methylene chloride: 0.15 mL methanol: 0.5 ml hexane); $^1\text{H NMR}$ (400 MHz, $\text{DMSO-}d_6$) δ 10.41 (s, 1H, NH D_2O exchangeable), 8.39 (s, 1H, NH D_2O exchangeable), 8.17 (s, 1H, pyrimidine H), 7.36 (m, 3H, ArH), 7.13 (m, 1H, ArH), 6.77 (m, 1H, ArH), 2.91 (s, 2H, cyclohexyl), 2.75 (s, 2H,

cyclohexyl), 1.81 (s, 4H, cyclohexyl); ^{13}C NMR (100 MHz, DMSO- d_6) δ 22.69, 22.91, 25.30, 25.88 (cyclohexyl), 115.49, 124.04, 124.63, 127.37, 129.21, 129.88, 131.42, 132.14, 139.00, 151.46, 153.34, 158.56, 161.42, 165.89, 166.23 (C=S); FT-IR (ν max, cm^{-1}): 3371, 3317 (2NH), 3055 (aromatic CH), 2927 (aliphatic CH); MS: (Mwt.: 340): m/z , 340.75 [M^+ , (25.15%)], 85.85 (100%). Anal. Calcd for $\text{C}_{17}\text{H}_{16}\text{N}_4\text{S}_2$: C, 59.97; H, 4.74; N, 16.46; Found: C, 60.23; H, 4.86; N, 16.73.

1-(5,6,7,8-Tetrahydrobenzo[4,5]thieno[2,3-d]pyrimidin-4-yl)-3-(m-tolyl)urea (9b) Light brown powder, m.p. 300 °C Yield: 85%; ($R_F=0.44$, Elution system: 1 mL of methylene chloride: 0.15 mL methanol: 0.5 mL hexane); ^1H NMR (400 MHz, DMSO- d_6) δ 11.23 (s, 1H, NH D_2O exchangeable), 8.71 (s, 1H, NH D_2O exchangeable), 8.28 (s, 1H, pyrimidine H), 7.43 (d, $J=8.3$ Hz, 1H, ArH), 7.24 (d, $J=7.2$ Hz, 1H, ArH), 6.91 (d, $J=7.5$ Hz, 2H, ArH), 3.05 (s, 3H, cyclohexyl), 2.84 (s, 2H, cyclohexyl), 2.31 (s, 3H, CH_3), 1.83 (s, 4H, cyclohexyl); ^{13}C NMR (100 MHz, DMSO- d_6) δ 21.67 (CH_3), 22.44, 22.69, 25.29, 25.89 (cyclohexyl), 115.77, 117.06, 119.12, 120.33, 122.94, 127.33, 129.03, 131.43, 138.38, 140.12, 153.32, 158.56, 165.91 (C=O); FT-IR (ν max, cm^{-1}): 3429, 3201 (2NH), 3028 (aromatic CH), 2978 (aliphatic CH), 1708 (C=O); MS: (Mwt.: 338): m/z , 338.30 [M^+ , (47.36%)], 262.84 (100%); Anal. Calcd for $\text{C}_{18}\text{H}_{18}\text{N}_4\text{O}_2\text{S}$: C, 63.88; H, 5.36; N, 16.56; O, 4.73; Found: C, 64.12; H, 5.49; N, 15.75.

1-(4-Chloro-3-(trifluoromethyl)phenyl)-3-(5,6,7,8-tetrahydrobenzo[4,5]thieno[2,3-d]pyrimidin-4-yl)urea (9c) Gray powder; m.p. 300 °C, Yield: 80%; ($R_F=0.33$, Elution system: 1 mL of methylene chloride: 0.15 mL methanol: 0.5 mL hexane) ^1H NMR (400 MHz, DMSO- d_6) 11.25 (s, 1H, NH, D_2O exchangeable), 8.17 (s, 1H, pyrimidine H), 7.26 (d, $J=8.6$ Hz, 1H, ArH), 6.99 (s, 1H, ArH), 6.78 (m, 2H, ArH, NH D_2O exchangeable), 2.90 (s, 2H, cyclohexyl), 2.74 (s, 2H, cyclohexyl), 1.81 (s, 4H, cyclohexyl). FT-IR (ν max, cm^{-1}): 3433, 3167 (2NH), 3039 (aromatic CH), 2947 (aliphatic CH), 1708 (C=O); MS: (Mwt.: 426): m/z , 426.46 [M^+ , (100%)], 428.35 [$\text{M}^+ + 2$, (17.14%)]. Anal. Calcd for: $\text{C}_{18}\text{H}_{18}\text{N}_4\text{O}_2\text{S}$: C, 50.65; H, 3.31; N, 13.13; Found: C, 50.89; H, 3.45; N, 13.41.

Biological assessment

In vitro GSK-3 β inhibitory assays

The assay was run to gauge the designed compounds' ability to inhibit GSK-3. The biochemical test Z'-LYTE A synthesized FRET-peptide receives the gamma-phosphate of ATP produced by the kinase during the main reaction at a single tyrosine, serine, or threonine residue. Non-phosphorylated FRET-peptides are found and degraded by a

site-specific protease in the secondary reaction. Development Reagent cleavage is prevented by FRET-peptide phosphorylation. While FRET is maintained by uncleaved, phosphorylated FRET-peptides, FRET between the donor (coumarin) and acceptor (fluorescein) fluorophores on the FRET-peptide is broken by cleavage. The radiometric approach, which quantifies reaction progress, determines the ratio (the Emission Ratio) of donor emission to acceptor emission following excitation of the donor fluorophore at 400 nm. By calculating how much ATP is still in solution after a kinase reaction, it quantifies kinase activity. The quantity of ATP present and the degree of kinase activity are both negatively connected with the luminous signal from the experiment.

Assay for anti-proliferative action against a range of NCI 60-cell lines in vitro

The NCI cancer screening procedure includes a comparison of all substances to the sixty NCI cell line panel representing leukemia, NSCLC, cell lines from breast cancer, prostate cancer, melanoma, CNS cancer, renal cancer, ovarian cancer, and colon cancer at a single point of 10 μM . The results of the single-dose screen can be presented using a mean graph.

Molecular modeling

Molecular docking

Protein preparation

The protein data bank was utilized to get the structure of the GSK3- β proteins, which has (PDB ID: *IJIB*). Partial charges were calculated and the enzymes were protonated. In the simulations, water molecules surrounding the cocrystallized ligands were deleted. The defined and isolated binding pocket was determined.

Ligand preparation

The following steps are taken by test ligand structures to prepare them for docking: The target molecules were created using ChemBioDraw Ultra 14.0, which was then repeated to MOE. (2) In three dimensions, the chemicals were protonated. (3) The constructions were built to use as little energy as possible The Merck Molecular Force Field produces a gradient of 0.5 (MMff94x). (4) Each molecule's force field partial charges were calculated. (5) Each molecule was subjected to a stochastic conformational analysis using default parameters, and the results were saved in a separate conformational database. (6) The most stable conformers of each molecule were recorded

in a separate database in order for each molecule to dock onto the active site of the androgen receptor.

In silico ADMET study

Measuring drug probability and pharmacokinetics properties is critical in the development of novel medications. The Swiss Institute of Bioinformatics' SWISSADME server, a free web service, our target compounds' physicochemical characteristics were computed using 'ADME characteristics, pharmacokinetic qualities, and druglike nature may all be predicted.

Supplementary Information

The online version contains supplementary material available at <https://doi.org/10.1186/s13065-023-01026-w>.

Additional file 1. supplementary material.

Acknowledgements

The authors express thanks to NCI, Maryland USA for carrying out cytotoxicity study.

Author contributions

K.A.M.A created the entire study, while H.S.I, E.Z.E supervised and approved the chemical work and the article's chemical work. J.S.S synthesized the compounds and this article was written by S.R.A.E and J.S.S. All of the authors reviewed the article.

Funding

Open access funding provided by The Science, Technology & Innovation Funding Authority (STDF) in cooperation with The Egyptian Knowledge Bank (EKB). This research did not receive any specific grant from funding agencies in the public, commercial, or not-for-profit sectors.

Availability of data and materials

All data generated or analyzed during this study are included in this published article (and its additional information files).

Declarations

Ethical approval and consent to participation

Not applicable.

Consent for publication

Not applicable.

Competing interests

The authors declare that they have no competing interests.

Author details

¹Department of Pharmaceutical Chemistry, Faculty of Pharmacy, Egyptian Russian University, P.O. Box 11829, Badr City, Cairo, Egypt. ²Department of Pharmaceutical Chemistry, Faculty of Pharmacy, Ain Shams University, P.O. Box 11566, Abbassia, Cairo, Egypt.

Received: 29 March 2023 Accepted: 29 August 2023

Published online: 27 September 2023

References

- Matthews HK, Bertoli C, de Bruin RAM. Cell cycle control in cancer. *Nat Rev Mol Cell Biol.* 2021;23(1):74–88. <https://doi.org/10.1038/s41580-021-00404-3>.

- Cell cycle. <https://www.genome.gov/genetics-glossary/Cell-Cycle>. Accessed 18 March 2023.
- Kannaiyan R, Mahadevan D. A comprehensive review of protein kinase inhibitors for cancer therapy. *Expert Rev Anticancer Ther.* 2018;18(12):1249–70. <https://doi.org/10.1080/14737140.2018.1527688>.
- Martinez A, Castro A, Dorronsoro I, Alonso M. Glycogen synthase kinase 3 (GSK-3) inhibitors as new promising drugs for diabetes, neurodegeneration, cancer, and inflammation. *Med Res Rev.* 2002;22(4):373–84. <https://doi.org/10.1002/MED.10011>.
- Augello G, Emma MR, Cusimano A, Azzolina A, Montalto G, McCubrey JA, Cervello M. The role of GSK-3 in cancer immunotherapy: GSK-3 inhibitors as a new frontier in cancer treatment. *Cells.* 2020;9:1427. <https://doi.org/10.3390/CELLS9061427>.
- Beurel E, Grieco SF, Jope RS. Glycogen synthase kinase-3 (GSK3): regulation, actions, and diseases. *Pharmacol Ther.* 2015;148:114–31. <https://doi.org/10.1016/J.PHARMTHERA.2014.11.016>.
- Tang YY, Sheng SY, Lu CG, Zhang YQ, Zou JY, Lei YY, Gu Y, Hong H. Effects of glycogen synthase kinase-3β inhibitor TWS119 on proliferation and cytokine production of TILs from human lung cancer. *J Immunother.* 2018;41(7):319–28. <https://doi.org/10.1097/JCI.0000000000000234>.
- Maeda Y, Nakano M, Sato H, Miyazaki Y, Schweiker SL, Smith JL, Truesdale AT. 4-Acylamino-6-arylfuro[2,3-d]pyrimidines: potent and selective glycogen synthase kinase-3 inhibitors. *Bioorg Med Chem Lett.* 2004;14(15):3907–11. <https://doi.org/10.1016/j.bmcl.2004.05.064>.
- US9090592B2 - Heterocyclic compounds and their use as glycogen synthase kinase-3 inhibitors—Google Patents. <https://patents.google.com/patent/US9090592B2/ko>. Accessed 24 Feb 2023.
- Boulahjar R, Ouach A, Bourg S, Bonnet P, Lozach O, Meijer L, Guguen-Guilouzo C, Le Guevel R, Lazar S, Akssira M, Troin Y, Guillaumet G, Routier S. Advances in tetrahydropyrido[1,2-a]isoindolone (valmerins) series: potent glycogen synthase kinase 3 and cyclin dependent kinase 5 inhibitors. *Eur J Med Chem.* 2015;101:274–87. <https://doi.org/10.1016/j.ejmech.2015.06.046>.
- Gould TD, Einat H, Bhat R, Manji HK. AR-A014418, a selective GSK-3 inhibitor, produces antidepressant-like effects in the forced swim test. *Int J Neuropsychopharmacol.* 2004;7(4):387–90. <https://doi.org/10.1017/S1461145704004535>.
- Sahin I, Eturi A, De Souza A, Pamarthy S, Tavora F, Giles FJ, Carneiro BA. (2019), "Glycogen synthase kinase-3 beta inhibitors as novel cancer treatments and modulators of antitumor immune responses." *Cancer Biol Ther.* 2019;20(8):1047–56. <https://doi.org/10.1080/15384047.2019.1595283>.
- Ogunleye AJ, Olanrewaju AJ, Arowosegbe M, Omotuyi OI. Molecular docking based screening analysis of GSK3B. *Bioinformation.* 2019;15(3):201–8. <https://doi.org/10.6062/97320630015201>.
- Babu PA, Chitti S, Rajesh B, Prasanth VV, Kishen JVR, Vali RK. In silico-based ligand design and docking studies of GSK-3β inhibitors. *Chem-Bio Inform J.* 2010;10(1):1–12. <https://doi.org/10.1273/CBIJ.10.1>.
- Quesada-Romero L, Mena-Ulecia K, Tiznado W, Caballero J. Insights into the interactions between maleimide derivatives and GSK3b combining molecular docking and QSAR. *PLoS ONE.* 2014;9(7):102212. <https://doi.org/10.1371/journal.pone.0102212>.
- Arciniegas Ruiz SM, Eldar-Finkelman H. Glycogen synthase kinase-3 inhibitors: preclinical and clinical focus on CNS-A decade onward. *Front Mol Neurosci.* 2022;14:349. <https://doi.org/10.3389/FNMOL.2021.792364>.
- Puterova Z, Krutošiková A, Véghe D. Gewald reaction: synthesis, properties and applications of substituted 2-aminothiophenes. *ARKIVOC.* 2010;2010(1):209–46. <https://doi.org/10.3998/ark.5550190.0011.105>.
- Meyer JF, Wagner EC. The Niementowski reaction. The use of methyl anthranilate or isatoic anhydride with substituted amides or amidines in the formation of 3-substituted-4-keto-3,4-dihydroquinazolines. the course of the reaction. *J Org Chem.* 2002;67(3):239–52. <https://doi.org/10.1021/jo01191a005>.
- Adel M, Serya RAT, Lasheen DS, Abouzid KAM. Identification of new pyrrolo[2,3-d]pyrimidines as potent VEGFR-2 tyrosine kinase inhibitors: design, synthesis, biological evaluation and molecular modeling. *Bioorg Chem.* 2018;81:612–29. <https://doi.org/10.1016/J.BIOORG.2018.09.001>.
- Abdel-Aziz HA, Elsamani T, Attia MI, Alanazi AM. The reaction of ethyl 2-oxo-2H-chromene-3-carboxylate with hydrazine hydrate. *Molecules.* 1985;18:2084–95. <https://doi.org/10.3390/molecules18022084>.

21. Tang J, Lv L, Dai X-J, Li C-C, Li L, Li C-J. Nickel-catalyzed cross-coupling of aldehydes with aryl halides via hydrazone intermediates. *Chem Commun.* 2018;54(14):1750–3. <https://doi.org/10.1039/C7CC09290C>.
22. Carping LA. Oxidative reactions of hydrazines. I. A new synthesis of acid chlorides. *J Am Chem Soc.* 1957;79(1):96–8. <https://doi.org/10.1021/JA01558A025/ASSET/JA01558A025>.
23. Burkus J. Tertiary amine catalysis of the reaction of phenyl isocyanate with alcohols. *J Org Chem.* 1961;26(3):779–82. <https://doi.org/10.1021/JO01062A032>.
24. Abd El Hadi SR, Lasheen DS, Hassan MA, Abouzid KAM. Design and synthesis of 4-anilinothieno[2,3-d]pyrimidine-based compounds as dual EGFR/HER-2 inhibitors. *Arch Pharm.* 2016;349(11):827–47. <https://doi.org/10.1002/ARDP.201600197>.
25. Nirogi RVS, Kambhampati SR, Kothmirkar P, Arepalli S, Pamuleti NRG, Shinde AK, Dubey PK. Convenient and efficient synthesis of some novel fused thieno pyrimidines using Gewald's reaction. *Synth Commun.* 2011;41(19):2835–51. <https://doi.org/10.1080/00397911.2010.515357>.
26. Azab ME, Ibraheem MAE, Madkour HMF. The utility of 2-(5,6,7,8-tetrahydrobenzo[b]thieno-[2,3-d]pyrimidin-4-yl)oxy) acetyl-drazide in heterocyclic synthesis. *Phosphorus Sulfur Silicon Relat Elem.* 2006;181(6):1299–313. <https://doi.org/10.1080/10426500500326834>.
27. Mahdavi B, Hosseini-Tabar SM, Rezaei-Seresht E, Rezaei-Seresht H, Falanji F. Synthesis and biological evaluation of novel hybrid compounds derived from gallic acid and the 2-aminothiophene derivatives. *J Iran Chem Soc.* 2020;17(4):809–15. <https://doi.org/10.1007/S13738-019-01813-0>.
28. Pfeiffer WD, Dollinger H, Langer P. Synthesis of 5-thioxo-hexahydrobenzo[b]thiopheno[2,3-d]-1,2,4-triazolo[1,5-c]pyrimidines and related compounds based on cyclocondensations of 2-isothiocyanato-3-cyano-4,5,6,7-tetrahydrobenzo[b]thiophene. *Phosphorus Sulfur Silicon Relat Elem.* 2009;184(3):626–37. <https://doi.org/10.1080/10426500802243216>.
29. Li W, Chu J, Fan T, Zhang W, Yao M, Ning Z, Wang M, Sun J, Zhao X, Wen A. Design and synthesis of novel 1-phenyl-3-(5-(pyrimidin-4-ylthio)-1,3,4-thiadiazol-2-yl)urea derivatives with potent anti-CML activity throughout PI3K/AKT signaling pathway. *Bioorg Med Chem Lett.* 2019;29(14):1831–5. <https://doi.org/10.1016/J.BMCL.2019.05.005>.

Publisher's Note

Springer Nature remains neutral with regard to jurisdictional claims in published maps and institutional affiliations.

Ready to submit your research? Choose BMC and benefit from:

- fast, convenient online submission
- thorough peer review by experienced researchers in your field
- rapid publication on acceptance
- support for research data, including large and complex data types
- gold Open Access which fosters wider collaboration and increased citations
- maximum visibility for your research: over 100M website views per year

At BMC, research is always in progress.

Learn more biomedcentral.com/submissions

